

Finite density QCD with chiral invariant four-fermion interactions

Michael Chavel*

Department of Physics, University of Illinois at Urbana,

1110 W. Green St, Urbana, IL 61801-3080

(April 20, 1997)

Abstract

A mean field analysis of finite density QCD is presented including the effects of additional chiral invariant four-fermion interactions. A lattice regularization is used with $N_f = 4$ flavors of staggered fermions. The use of the four-fermion coupling as an improved extrapolation parameter over the bare quark mass in Monte Carlo simulations is discussed. Particular attention is given to the structure of the phase diagram and the order of the chiral phase transition. At zero gauge coupling, the model reduces to a Nambu–Jona-Lasinio model. In this limit the chiral phase transition is found to be second-order near the zero-density critical point and otherwise first-order. In the strong gauge coupling limit a first-order chiral phase transition is found. In this limit the additional four-fermion interactions do not qualitatively change the physics. The results agree with previous studies of QCD as the four-fermion coupling vanishes.

12.38.Gc, 11.30.Rd

Typeset using REVTeX

*E-mail: chavel@uiuc.edu

I. INTRODUCTION

Monte Carlo simulations of lattice gauge theories with dynamical fermions become very computationally intensive at small fermion masses due to the zero mass singularity of the Dirac operator. In order to study theories with light fermions it becomes necessary to carry out simulations with relatively large bare masses, and then extrapolate back to lower values. In studying models with chiral symmetry or dynamical chiral symmetry breaking it would be desirable to simulate the models directly in the chiral limit, without having to introduce any bare mass terms which explicitly break the symmetry.

A new approach to this problem has been suggested [1–3] which does not explicitly break chiral symmetry. The idea is to add additional terms to the lattice action, corresponding to chiral invariant four-fermion interactions. In the continuum limit, as the lattice spacing reduces to zero, these additional terms are irrelevant [4] (in the renormalization group sense). However, at finite lattice spacings they favor the generation of a dynamical fermion mass. This dynamical mass removes the singularity in the Dirac operator allowing for simulations with exactly zero bare fermion masses [2,3].

One particular area where this may soon lead to significant progress is in the study of QCD at finite density. It is generally expected that at some density greater than that of normal nuclear matter there is a transition to a quark-gluon plasma and chiral symmetry is restored. The nature and order of this transition may be an important factor in cosmological models, neutron stars, and future heavy ion collision experiments. Mean field calculations at both infinite [5,6] and strong [7,8] gauge coupling indicate that the transition is first-order at low temperatures. Unfortunately, Monte Carlo simulations of QCD at non-zero density have not been able to give a physically accurate description of the transition [6,9].

Quenched simulations of QCD using the grand canonical formulation [6] show the transition at a value of the chemical potential equal to one half the pion mass, vanishing as the bare quark mass $m_0 \rightarrow 0$. These results are now understood [10] to correspond to the $N_f \rightarrow 0$ limit of a theory of N_f quarks with regular action and N_f quarks with the conjugate action, and are therefore unrelated to QCD.

Unquenched Monte Carlo calculations have to deal with a complex fermionic determinant due to the introduction of the chemical potential. Hence, conventional Monte Carlo algorithms can not be applied. Some results have been obtained at infinite gauge coupling by representing the partition function in terms of monomers, dimers, and baryonic loops [11], and also on small lattices, by using a spectral density method [12]. The results are consistent with mean field calculations. However, it is not clear how to extend these methods to intermediate or weak gauge coupling.

The evaluation of the complex determinant can also be avoided by the fugacity expansion method of Refs. [13,14]. However, the proper physics of chiral symmetry breaking, with a massless pion, has not yet been achieved using finite quark masses with this method [9]. Simulations of zero mass QCD with additional chiral four-fermion interactions, called χ QCD [3], may be able to overcome this problem. In support of this approach, this paper presents a mean field analysis of χ QCD at non-zero density. The calculations will be restricted to the two limiting cases of zero and infinite gauge coupling. No restrictions are placed the strength of the four fermion interactions. Although in applications approximating QCD they should be chosen relatively weak.

II. THE χ QCD MODEL

The χ QCD action, using the staggered fermion [15] formulation, is

$$\begin{aligned}
S &= S_f + S_g, \\
S_f &= \frac{N_f}{8} \gamma \sum_{\tilde{x}} (\sigma^2(\tilde{x}) + \pi^2(\tilde{x})) \\
&\quad + \sum_{a=1}^{N_f/4} \left[\sum_{x,y} \bar{\chi}_i^a(x) \mathcal{M}^{ij}(x,y) \chi_j^a(y) + \frac{1}{16} \sum_x \bar{\chi}_i^a(x) \chi_i^a(x) \sum_{\langle \tilde{x}, x \rangle} (\sigma(\tilde{x}) + i\varepsilon(x)\pi(\tilde{x})) \right], \\
S_g &= -\beta \sum_{\square} \left[1 - \frac{1}{N} \text{Re}(\text{Tr}_{\square} UUUU) \right].
\end{aligned} \tag{1}$$

$\bar{\chi}_i^a$ and χ_i^a are complex Grassmannian fields defined on each site of the lattice. Each χ_i^a represents four degenerate flavors of fermions, so the sum over the flavor index a runs from 1 to $N_f/4$. We are interested in studying QCD, however, the calculations can be done for any $SU(N)$ gauge group. Considering this more general case, the color indices i, j run from 1 to N .

The fermion hopping matrix $\mathcal{M}^{ij}(x, y)$ is given by

$$\mathcal{M}^{ij}(x, y) = \frac{1}{2} \sum_{\nu=0}^3 \left[f_{\nu}(x) U_{\nu}^{ij}(x) \delta_{y, x+\hat{\nu}} - f_{\nu}^{-1}(x) U_{\nu}^{ij}(x - \hat{\nu}) \delta_{y, x-\hat{\nu}} \right] + m_0 \delta_{y,x}, \tag{2}$$

with

$$f_{\nu}(x) \equiv \begin{cases} \exp(\mu) & \nu = 0 \\ \eta_{\nu}(x) & \nu = 1, 2, 3 \end{cases}. \tag{3}$$

Here μ is the chemical potential [16,6] measured in units of the lattice spacing. The $\eta_{\nu}(x)$ are the conventional Kawamoto-Smit [17] phases $(-1)^{x_0+\dots+x_{\nu-1}}$. m_0 is the bare (current) mass of the quarks which can be set to zero, but is included here for completeness.

The auxiliary fields σ and π have been introduced to separate the four-fermion interactions [18,19]. They are defined on the dual lattice. The symbol $\langle \tilde{x}, x \rangle$ represents the 16 dual sites \tilde{x} adjacent to the direct lattice site x . $\varepsilon(x)$ represents the alternating phase $(-1)^{x_0+x_1+x_2+x_3}$. After integrating over the auxiliary fields, the lattice model approximates the continuum theory

$$\mathcal{L} = \bar{\psi} (\not{D} + \mu\gamma_0 + m_0) \psi - \frac{G}{2N_f/4} [(\bar{\psi}\psi)^2 - (\bar{\psi}\gamma_5\psi)^2] - \frac{1}{2g^2} \text{Tr}(F_{\mu\nu}F^{\mu\nu}), \tag{4}$$

with $G=1/\gamma$ and $2N/g^2=\beta$. (The spinor, color and flavor indices have been suppressed.)

In the chiral limit ($m_0=0$), the continuum theory (4) is invariant under the global $U(1)$ chiral symmetry

$$\bar{\psi} \mapsto \bar{\psi} e^{i\gamma_5\theta}, \quad \psi \mapsto e^{i\gamma_5\theta} \psi. \tag{5}$$

In the language of the lattice model this translates to

$$\bar{\chi}^a \mapsto \bar{\chi}^a e^{i\theta\varepsilon(x)}, \quad \chi^a \mapsto e^{i\theta\varepsilon(x)} \chi^a, \quad \text{and} \quad \begin{pmatrix} \sigma \\ \pi \end{pmatrix} \mapsto \begin{pmatrix} \cos(2\theta) & \sin(2\theta) \\ -\sin(2\theta) & \cos(2\theta) \end{pmatrix} \begin{pmatrix} \sigma \\ \pi \end{pmatrix}. \quad (6)$$

The U(1) chiral symmetry is spontaneously broken in the low density hadron phase through the dynamics of the color gauge fields. The chiral condensate

$$\langle \bar{\chi}^a \chi^a \rangle = \frac{N_f}{4} \gamma \langle \sigma \rangle, \quad (7)$$

is nonzero in the broken phase, and serves as the order parameter for the chiral phase transition.

III. ZERO GAUGE COUPLING — NJL LIMIT

As the gauge coupling vanishes χ QCD reduces to a lattice Nambu–Jona-Lasinio (NJL) model [20]. In Ref. [21] the three dimensional version of this model was studied at non-zero chemical potential in a $1/N_f$ expansion. Presented here are results for four dimensions. Of particular interest is the structure of the finite density phase diagram and the order of the chiral phase transition.

When $\beta \rightarrow \infty$ the SU(N) gauge variables are frozen to $U_\nu^{ij}(x) = \delta^{ij}$ at each link of the lattice. Gaussian integration over the fermion fields leaves the following, bosonic, partition function

$$Z = \int D\sigma D\pi \exp\left\{-\frac{N_f}{8} \gamma \sum_{\tilde{x}} (\sigma^2(\tilde{x}) + \pi^2(\tilde{x})) + \frac{N \cdot N_f}{4} \text{Tr} \ln[S_F^{-1}]\right\}, \quad (8)$$

where

$$S_F^{-1}(x, y) = \frac{1}{2} \sum_{\nu=0}^3 \left[f_\nu(x) \delta_{y, x+\hat{\nu}} - f_\nu^{-1}(x) \delta_{y, x-\hat{\nu}} \right] + m_0 + \frac{1}{16} \sum_{\langle \tilde{x}, x \rangle} (\sigma(\tilde{x}) + i\varepsilon(x)\pi(\tilde{x})). \quad (9)$$

The mean field, saddle point solution $\{\bar{\sigma}, \bar{\pi}\}$ (equivalent to the first order of a large N_f expansion) is given by the “gap equation”

$$\begin{pmatrix} \bar{\sigma} \\ \bar{\pi} \end{pmatrix} \gamma = \begin{pmatrix} \bar{\sigma} + m_0 \\ \bar{\pi} \end{pmatrix} N \text{Tr}[S_F], \quad (10)$$

where (in the infinite volume limit)

$$\text{Tr}[S_F] = 16 \int_{-\frac{\pi}{2}}^{\frac{\pi}{2}} \frac{d^4 k}{(2\pi)^4} \frac{1}{\frac{1}{2}(1 - \cos 2k_0 \cosh 2\mu - i \sin 2k_0 \sinh 2\mu) + \sum_{\nu=1,2,3} \sin^2 k_\nu + m^2}, \quad (11)$$

$$m^2 = (\bar{\sigma} + m_0)^2 + \bar{\pi}^2.$$

Here m is the effective (dynamical) mass of the quarks. If the bare quark mass m_0 is non-zero, chiral symmetry is broken explicitly. The unique solution is then identified with $\bar{\sigma} > 0$ and $\bar{\pi} = 0$. In the chiral limit the solution is invariant under the transformation (6), and so we are free to choose $\bar{\pi} = 0$. This is the case of interest, which we will now discuss for $N = 3$.

The gap equation is easily evaluated numerically on a finite size lattice by replacing the momentum integrations with discrete sums [21]. A $(48)^4$ Euclidean lattice was found to be sufficiently large to eliminate finite-size effects. Figure 1 shows the resulting behavior of $\bar{\sigma}$ at zero chemical potential. The other data points show (zero mass) measurements of $\sqrt{\sigma^2 + \pi^2}$ from Monte Carlo simulations of χ QCD in the $\beta \rightarrow \infty$ limit [22]. The mean field phase transition is at $\gamma_c = 1.86$. This is also in agreement with Monte Carlo simulations of the pure NJL model [23], where the transition was found at $\gamma_c = 1.81$ ($\gamma_c/N \Leftrightarrow \beta_c$ in their notation).

At non-zero chemical potential the chiral phase transition is given by setting $\bar{\sigma} = 0$. The gap equation then produces the critical line shown in the phase diagram of Fig. 2. The upper left section of the phase diagram corresponds to the spontaneously broken symmetry phase, with $\bar{\sigma} > 0$. The remainder of the diagram represents the chiral symmetric phase, with $\bar{\sigma} = 0$.

As an alternative to solving (10) the minimum energy solution can be found by a direct evaluation of the action. This also allows for a clearer determination of the order of the chiral phase transition. Substituting the uniform ansatz $\{\bar{\sigma}, 0\}$ into the action and Fourier transforming one finds

$$\bar{S} = \frac{1}{2}\gamma\bar{\sigma}^2 - 3 \cdot 16 \int_{-\frac{\pi}{2}}^{\frac{\pi}{2}} \frac{d^4k}{(2\pi)^4} \ln \left[\frac{1}{2}(1 - \cos 2k_0 \cosh 2\mu - i \sin 2k_0 \sinh 2\mu) + \sum_{\nu=1,2,3} \sin^2 k_\nu + \bar{\sigma}^2 \right]. \quad (12)$$

Figure 4 contains plots of \bar{S} as a function of $\bar{\sigma}$ at $\gamma=1$. Each line corresponds to a different value of the chemical potential. The plots have been rescaled so that \bar{S} is zero at $\bar{\sigma} = 0$. The figure shows a clear first-order (discontinuous) transition as the chemical potential is increased from zero. However, at larger values of γ the transition becomes continuous, as shown in Fig. 3 for $\gamma=1.5$. The chiral transition remains continuous as the critical line is followed towards $\mu=0$. This appears consistent with the second-order transition found in the $1/N_f$ expansion at zero-density [23].¹ What is perhaps unanticipated is that the second-order transition actually extends into the interior of the phase diagram for small values of the chemical potential.

The behavior of $\bar{\sigma}$ as a function of the chemical potential is plotted in Fig. 5, for the fixed values of $\gamma=1$ and 1.5. Other quantities of interest include the quark number density and quark energy density.

$$\begin{aligned} \langle \psi^\dagger \psi \rangle &= -\frac{\partial \ln Z}{\partial \mu} \\ &= -N \text{Tr} \left[\frac{\partial S_F^{-1}}{\partial \mu} S_F \right] \end{aligned}$$

¹ Monte Carlo calculations [23] indicate that the theory is in fact trivial, exhibiting logarithmic scaling corrections to mean field exponents.

$$\begin{aligned}
&= 3 \cdot 16 \int_{-\frac{\pi}{2}}^{\frac{\pi}{2}} \frac{d^4 k}{(2\pi)^4} \frac{\frac{1}{2}(\cos 2k_0 \sinh 2\mu + i \sin 2k_0 \cosh 2\mu)}{\frac{1}{2}(1 - \cos 2k_0 \cosh 2\mu - i \sin 2k_0 \sinh 2\mu) + \sum_{\nu=1,2,3} \sin^2 k_\nu + \bar{\sigma}^2}, \\
\langle \psi^\dagger \partial_0 \psi \rangle &= N \text{Tr}[(S_F^{-1})^0 S_F] \\
&= 3 \cdot 16 \int_{-\frac{\pi}{2}}^{\frac{\pi}{2}} \frac{d^4 k}{(2\pi)^4} \frac{\frac{1}{2}(1 - \cos 2k_0 \cosh 2\mu - i \sin 2k_0 \sinh 2\mu)}{\frac{1}{2}(1 - \cos 2k_0 \cosh 2\mu - i \sin 2k_0 \sinh 2\mu) + \sum_{\nu=1,2,3} \sin^2 k_\nu + \bar{\sigma}^2}. \quad (13)
\end{aligned}$$

These are plotted in Fig. 6 and Fig. 7, respectively, for the values of $\gamma = 1$ and 1.5. As expected, the quark density is essentially zero in the broken phase. As the chemical potential is increased towards the critical value separating the two phases, roughly equal to $m = \bar{\sigma}$, the order parameter begins to decrease and the density rises. At the chiral transition the quark mass abruptly vanishes. Hence, the quark density abruptly increases. In the symmetric phase, the number density increases $\sim \mu^3$ at low densities, which is consistent with a non-interacting quark gas. As the lattice becomes filled the density eventually saturates at the maximum value allowed by the Pauli exclusion principle, of $N=3$.

IV. THE STRONG GAUGE COUPLING LIMIT

In the previous section we studied the case where the gauge coupling vanished. However, in using χ QCD to approximate QCD one is really interested in the case where the four-fermion interactions are very weak compared to the gauge interactions; naively when $G \ll g$. In this section we will study the strong gauge coupling limit of $g \rightarrow \infty$. Similar infinite gauge coupling calculations have been carried out in [24], as well as in [5,6] at finite density. Some of the same techniques will be used here with suitable modifications.

Begin by defining the following ‘‘meson’’ and ‘‘baryon’’ fields:

$$\begin{aligned}
M^{ab}(x) &\equiv \bar{\chi}_i^a(x) \chi_i^b(x), \\
\bar{B}^{ab\dots c}(x) &\equiv \frac{1}{N!} \epsilon_{ij\dots k} \bar{\chi}_i^a(x) \bar{\chi}_j^b(x) \dots \bar{\chi}_k^c(x), \\
B^{ab\dots c}(x) &\equiv \frac{1}{N!} \epsilon_{ij\dots k} \chi_i^a(x) \chi_j^b(x) \dots \chi_k^c(x). \quad (14)
\end{aligned}$$

The meson fields commute for any value of N , while the baryon fields will anticommute (commute) for N odd (even).

At infinite gauge coupling ($\beta=0$) the gauge term in the action S_g is zero. Therefore, the gauge variables on each link are completely independent. Integrating over the $SU(N)$ gauge group at each link yields²

$$Z = \int D\bar{\chi} D\chi D\sigma D\pi$$

² Equation (15) is valid only for $N \geq 3$. Similar expressions for the $U(1)$ and $SU(2)$ gauge groups can be found in Ref. [24]

$$\begin{aligned}
& \times \exp \left\{ -\frac{N_f}{8} \gamma \sum_{\tilde{x}} (\sigma^2(\tilde{x}) + \pi^2(\tilde{x})) - \sum_{a=1}^{N_f/4} \sum_x \bar{\chi}_i^a(x) \chi_i^a(x) \left[m_0 + \frac{1}{16} \sum_{\langle \tilde{x}, x \rangle} (\sigma(\tilde{x}) + i\varepsilon(x)\pi(\tilde{x})) \right] \right\} \\
& \times \prod_x \prod_{\nu=0}^3 \left[1 + \frac{1}{4N} \text{Tr}_f [M(x)M(x+\tilde{\nu})] \right. \\
& \quad + \frac{1}{32N(N^2-1)} \left(\text{Tr}_f [M(x)M(x+\tilde{\nu})]^2 + N \text{Tr}_f [M(x)M(x+\tilde{\nu})M(x)M(x+\tilde{\nu})] \right) + \dots \\
& \quad \left. - \frac{(-1)^{N(N+1)/2}}{2^N} \left(f_\nu^N(x) \text{Tr}_f [\bar{B}(x)B(x+\tilde{\nu})] + (-1)^N f_\nu^{-N}(x) \text{Tr}_f [\bar{B}(x+\tilde{\nu})B(x)] \right) \right]. \quad (15)
\end{aligned}$$

Here Tr_f is the trace over flavor indices only. In writing (15), the full expression for the meson contributions has been truncated. (In general the series will terminate after terms of order $O(M^{NN_f/2})$ due to the Grassmannian nature of the χ_i^a fields.) For the remainder of the calculation we only need to retain the first meson-meson term. As shown in [24] this is consistent with a systematic expansion in $1/d$, where d is the number of space-time dimensions.

Exponentiating the product at each lattice site yields the following action:

$$\begin{aligned}
S = & \frac{N_f}{8} \gamma \sum_{\tilde{x}} (\sigma^2(\tilde{x}) + \pi^2(\tilde{x})) + \sum_x \text{Tr}_f [M(x)] \left(m_0 + \frac{1}{16} \sum_{\langle \tilde{x}, x \rangle} (\sigma(\tilde{x}) + i\varepsilon(x)\pi(\tilde{x})) \right) \\
& - \sum_{x,y} \left(\frac{1}{2} \text{Tr}_f [M(x)V(x,y)M(y)] + \text{Tr}_f [\bar{B}(x)V_B(x,y)B(y)] \right), \quad (16)
\end{aligned}$$

with

$$V(x,y) \equiv \frac{1}{4N} \sum_{\nu=0}^3 (\delta_{y,x+\tilde{\nu}} + \delta_{y,x-\tilde{\nu}}), \quad (17)$$

$$V_B(x,y) \equiv \frac{(-1)^{N(N+1)/2}}{2^N} \sum_{\nu=0}^3 (f_\nu^N(x) \delta_{y,x+\tilde{\nu}} + (-1)^N f_\nu^{-N} \delta_{y,x-\tilde{\nu}}). \quad (18)$$

Note that all the dependence on the chemical potential is now contained in $V_B(x,y)$.

We want to construct an effective action by integrating out the staggered fermion fields, as was done in the pure NJL case. To facilitate this we first linearize the action in the meson and baryon terms using the following identities:

$$\begin{aligned}
& \exp \left\{ \sum_{x,y} \frac{1}{2} \text{Tr}_f [M(x)V(x,y)M(y)] \right\} \\
& = \det[V] \int D\rho \exp \left\{ - \sum_{x,y} \frac{1}{2} \text{Tr}_f [\rho(x)V^{-1}(x,y)\rho(y)] - \sum_x \rho^{ab}(x)M^{ab}(x) \right\}, \quad (19)
\end{aligned}$$

$$\begin{aligned}
& \exp \left\{ \sum_{x,y} \text{Tr}_f [\bar{B}(x)V_B(x,y)B(y)] \right\} \\
& = \det[V_B] \int D\bar{b}Db \exp \left\{ - \sum_{x,y} \text{Tr}_f [\bar{b}(x)V_B^{-1}(x,y)b(y)] \right\} \\
& \quad \times \exp \left\{ - \sum_x (\bar{b}^{ab\dots c}(x)B^{ab\dots c}(x) + \bar{B}^{ab\dots c}(x)b^{ab\dots c}(x)) \right\}. \quad (20)
\end{aligned}$$

In writing the second identity we have taken N to be odd, as it is for QCD. In either case, the final expression for the effective action (26) will be correct for all $N \geq 3$.³

Let us now restrict the remainder of the calculation to $N_f = 4$ flavors which is technically much easier to handle. (Unlike the high temperature transition (at low density), the finite density transition should not have a large flavor dependence at low temperatures [7].) Integrating over $\bar{\chi}_i^a$ and χ_i^a we then find

$$\begin{aligned} Z = & \int D\sigma D\pi D\rho D\bar{b}Db \exp\left\{-\frac{1}{8}\gamma \sum_{\tilde{x}}(\sigma^2(\tilde{x}) + \pi^2(\tilde{x}))\right\} \det[V] \det[V_B] \\ & \times \det\left[\left(\rho(x) + m_0 + \frac{1}{16} \sum_{\langle\tilde{x},x\rangle} (\sigma(\tilde{x}) + i\varepsilon(x)\pi(\tilde{x}))\right)^N + (-1)^{\frac{N(N-1)}{2}} \bar{b}(x)b(x)\right] \\ & \times \exp\left\{-\sum_{x,y}\left[\frac{1}{2}\rho(x)V^{-1}(x,y)\rho(y) + \bar{b}(x)V_B^{-1}(x,y)b(y)\right]\right\}. \end{aligned} \quad (21)$$

Since $\det[V]$ does not depend upon any of the fields or the chemical potential, it can be dropped without affecting the calculation of any physical quantities. The remaining functional determinants can be exponentiated up into the action, producing an effective action

$$\begin{aligned} S_{eff} = & \frac{1}{2}\gamma \sum_{\tilde{x}}(\sigma^2(\tilde{x}) + \pi^2(\tilde{x})) + \sum_{x,y}\left(\frac{1}{2}\rho(x)V^{-1}(x,y)\rho(y) + \bar{b}(x)V_B^{-1}(x,y)b(y)\right) \\ & - \text{Tr} \ln[\Sigma^N(x) + (-1)^{\frac{N(N-1)}{2}} \bar{b}b] - \text{Tr} \ln[V_B], \end{aligned} \quad (22)$$

with

$$\Sigma(x) \equiv \rho(x) + m_0 + \frac{1}{16} \sum_{\langle\tilde{x},x\rangle} (\sigma(\tilde{x}) + i\varepsilon(x)\pi(\tilde{x})). \quad (23)$$

Using the fact that $\ln[1 + \frac{\bar{b}b}{\Sigma}] = \frac{\bar{b}b}{\Sigma}$ for the Grassmannian fields \bar{b} and b , (22) can be further simplified to

$$\begin{aligned} S_{eff} = & \frac{1}{2}\gamma \sum_{\tilde{x}}(\sigma^2(\tilde{x}) + \pi^2(\tilde{x})) + \sum_{x,y}\left(\frac{1}{2}\rho(x)V^{-1}(x,y)\rho(y) + \bar{b}(x)S_b^{-1}(x,y)b(y)\right) \\ & - \text{Tr} \ln[\Sigma^N(x)] - \text{Tr} \ln[V_B], \end{aligned} \quad (24)$$

with

$$S_b^{-1}(x,y) = V_B^{-1}(x,y) + \frac{\delta(x,y)}{\Sigma(x)^N}. \quad (25)$$

Integrating over \bar{b} and b , which are now just Gaussian integrals, we arrive at a final expression for the effective action at $\beta=0$

³ For N even $\det[V_B]$ is replaced by $\det[V_B^{-1}]$ in (20). Integration over \bar{b}, b in (21) then gives $\int D\bar{b}Db \bar{b}b e^{-\bar{b}V_B^{-1}b} = \det[V_B^2]$. Combining all the determinants eventually yields equation (26).

$$S_{eff} = \frac{1}{2}\gamma \sum_{\tilde{x}} (\sigma^2(\tilde{x}) + \pi^2(\tilde{x})) + \sum_{x,y} \frac{1}{2}\rho(x)V^{-1}(x,y)\rho(y) - \text{Tr} \ln[\Sigma^N(x) + V_B(x,y)]. \quad (26)$$

Now consider a uniform (mean field) saddle point approximation to the action. Denote the saddle point solution which minimizes the effective action by $\{\bar{\rho}, \bar{\sigma}, \bar{\pi}\}$. Substituting this into (26) and transforming to momentum space yields

$$\begin{aligned} \bar{S}_{eff} = \frac{1}{2}\gamma(\bar{\sigma}^2 + \bar{\pi}^2) + \frac{N}{4}\bar{\rho}^2 - 8 \int_{-\frac{\pi}{2}}^{\frac{\pi}{2}} \frac{d^4k}{(2\pi)^4} \ln \left[\frac{1}{2}(1 - \cos 2k_0 \cosh 2N\mu - i \sin 2k_0 \sinh 2N\mu) \right. \\ \left. + \sum_{\nu=1,2,3} \sin^2 k_\nu + m_B^2 \right], \end{aligned} \quad (27)$$

with

$$m_B^2 = 4^{N-1}[(\bar{\rho} + \bar{\sigma} + m_0)^2 + \bar{\pi}^2]^N. \quad (28)$$

\bar{S}_{eff} can be evaluated by an explicit summation over discrete momenta on a finite sized lattice, as carried out in section III. In the chiral limit ($m_0=0$) we find two distinct phases: For $\mu < \mu_c(\gamma)$ there is a spontaneously broken phase with⁴

$$\bar{\rho} = \sqrt{\frac{2}{1 + \frac{N}{2\gamma}}}, \quad \bar{\sigma} = \frac{N}{2\gamma}\bar{\rho}, \quad \bar{\pi} = 0; \quad (29)$$

while for $\mu > \mu_c(\gamma)$ there is a chiral symmetric phase, characterized by

$$\bar{\rho} = \bar{\sigma} = \bar{\pi} = 0. \quad (30)$$

(The same solutions are produced by evaluating the ‘‘gap equation’’, obtained by minimizing (27) with respect to $\{\bar{\rho}, \bar{\sigma}, \bar{\pi}\}$.) Notice that within each phase all of the order parameters are independent of the value of the chemical potential. Therefore, the chiral phase transition is discontinuous (first-order) for all values of γ . The critical line can be determined by setting $\bar{S}_{eff}(\{\bar{\rho}, \bar{\sigma}, \bar{\pi}\}; \mu_c) = \bar{S}_{eff}(\{0, 0, 0\}; \mu_c)$. This yields

$$\mu_c(\gamma) = \frac{1}{2} \ln[4(2 + N/\gamma)] - \frac{1}{2}, \quad (31)$$

in agreement with previous mean field QCD calculations [6,8] as $\gamma \rightarrow \infty$.

Let us now discuss the specific gauge group SU(3). The phase diagram is shown in Fig. 8. As expected, the values of μ_c increase monotonically as $G=1/\gamma$ increases. Of course, since $g \gg G$, chiral symmetry breaking is still due to the strong gauge (color) forces as in ordinary QCD. The additional four-fermion interactions merely enhance the effect. (This is clearly demonstrated by comparing Fig. 8 with the phase diagram produced in the absence of the gauge fields (Fig. 2).) The mean field chiral condensate is given by

⁴ Since the values of $\{\bar{\rho}, \bar{\sigma}, \bar{\pi}\}$ are independent of μ in each phase the analytic expressions (29) can be obtained with $\mu=0$. In which case, the baryon terms can be safely ignored [6] and $V_B(x,y)$ can be set equal to zero.

$$\langle \bar{\chi}\chi \rangle = \gamma \bar{\sigma} = \frac{3}{2} \bar{\rho}. \quad (32)$$

Values of $\bar{\rho}$ and $\bar{\sigma}$ in the broken phase are plotted as a function of $G=1/\gamma$ in Fig. 9. Included for comparison are values of σ from exploratory Monte Carlo simulations of χ QCD [22] at $\beta = 0.5$ and zero chemical potential.

Plots of the effective action for $\gamma \rightarrow \infty$ are shown in Fig. 10 at selected values of the chemical potential μ . It should be obvious from the figure that the chiral phase transition is indeed discontinuous, and that $\bar{\rho}$ does not depend on the value of the chemical potential within the broken phase. The value of $\mu_c=0.54$ agrees with the mean field result of [6] for ordinary QCD. Figure 11 contains similar plots of the effective action for $\gamma=1$. Notice that the general behavior of the action and the order of the transition remain unchanged. (This was explicitly checked for values down to $\gamma=.01$.)

Let us now consider the mass of the baryons in the broken phase. By adding baryon source terms to the original action, it is straightforward to show that the staggered baryon propagator $\langle \bar{B}(x)B(y) \rangle$ has the same pole structure as $S_b(x, y)$, defined in (25). Defining the baryon mass $M_B(\mu)$ to be the location of the pole of $\langle \bar{B}(x)B(y) \rangle$ in the broken phase gives

$$M_B(\mu) = \sinh^{-1}(m_B) - N\mu = \sinh^{-1}\left(4\left(2 + \frac{3}{\gamma}\right)^{\frac{3}{2}}\right) - 3\mu. \quad (33)$$

In the symmetric phase the dynamical quark mass vanishes along with the chiral order parameter. The pole in $\langle \bar{B}(x)B(y) \rangle$ disappears, and so, as expected we no longer have stable nuclear matter.

$M_B(\mu)$ is plotted in Fig. 12 for various values of γ . Notice that the chiral symmetry restoration occurs consistently at a value of $M_B(\mu_c)=3/2$. This value can be traced back to the first two terms of \bar{S}_{eff} in (27), which represents the mean field energy density of the chiral condensate. At weaker gauge coupling, where the binding energy is small, one would expect the phase transition to be closer to the baryon mass threshold $M_B(\mu_c)=0$ [6]. In ordinary QCD, one finds that this energy difference does indeed decrease when $1/g^2$ corrections are added to the calculations [8].

The quark number density and quark energy density are given by the following equations:

$$\begin{aligned} \langle \psi^\dagger \psi \rangle &= -\text{Tr} \left[\frac{\frac{\partial V_B}{\partial \mu}}{\Sigma^N + V_B} \right] \\ &= 3 \cdot 16 \int_{-\frac{\pi}{2}}^{\frac{\pi}{2}} \frac{d^4 k}{(2\pi)^4} \frac{\frac{1}{2}(\cos 2k_0 \sinh 2N\mu + i \sin 2k_0 \cosh 2N\mu)}{\frac{1}{2}(1 - \cos 2k_0 \cosh 2N\mu - i \sin 2k_0 \sinh 2N\mu) + \sum_{\nu=1,2,3} \sin^2 k_\nu + m_B^2}, \end{aligned} \quad (34)$$

$$\begin{aligned} \langle \psi^\dagger \partial_0 \psi \rangle &= \text{Tr} \left[\frac{(V_B)^0}{\Sigma^N + V_B} \right] \\ &= 16 \int_{-\frac{\pi}{2}}^{\frac{\pi}{2}} \frac{d^4 k}{(2\pi)^4} \frac{\frac{1}{2}(1 - \cos 2k_0 \cosh 2N\mu - i \sin 2k_0 \sinh 2N\mu)}{\frac{1}{2}(1 - \cos 2k_0 \cosh 2N\mu - i \sin 2k_0 \sinh 2N\mu) + \sum_{\nu=1,2,3} \sin^2 k_\nu + m_B^2}. \end{aligned} \quad (35)$$

In the broken phase the baryon mass gap remains relatively large all the way to the phase boundary. Therefore, the baryon density is strictly zero. In the symmetric phase the binding

energy of the quark matter is very large at strong coupling. Hence, the density jumps directly to saturation as the chemical potential is increased through the transition. This is certainly an artifact of working at infinite gauge coupling. Similar behavior has been found in other infinite coupling calculations [7].

V. ACKNOWLEDGMENTS

The author would like to thank John B. Kogut for suggesting this study and for providing the Monte Carlo data presented in Figs. 1 and 9.

REFERENCES

- [1] R. C. Brower, Y. Shen and C.-I. Tan, *Int. J. of Mod. Phys. C* **6**, 743 (1995).
- [2] J.B. Kogut and D.K. Sinclair, *Nucl. Phys. B (Proc. Suppl.)* **53**, 272 (1997).
- [3] I.M. Barbour, S.E. Morrison, and J.B. Kogut, hep-lat/9612012.
- [4] K.G. Wilson and J. Kogut, *Phys. Rep. C* **12**, 75 (1974).
- [5] P.H. Damgaard, D. Hochberg, and N. Kawamoto, *Phys. Lett.* **158B**, 239 (1985)
- [6] I. Barbour *et al.*, *Nucl. Phys.* **B275**, 296 (1986).
- [7] N. Bilić, F. Karsch, and K. Redlich, *Phys. Rev. D* **45**, 3228 (1992).
- [8] N. Bilić, K. Demeterfi, and B. Petersson, *Nucl. Phys.* **B377**, 651 (1992).
- [9] I.M. Barbour, J.B. Kogut and S.E. Morrison, *Nucl. Phys. B (Proc. Suppl.)* **53**, 456 (1997).
- [10] M.A. Stephanov, *Phys. Rev. Lett.* **76**, 4472 (1996).
- [11] F. Karsch and K.-H. Mütter, *Nucl. Phys.* **B313**, 541 (1989).
- [12] A. Gocksch, *Phys. Rev. Lett.* **61**, 2054 (1988).
- [13] P. Gibbs, *Phys. Lett.* **172B**, 53 (1986); *Phys. Lett.* **182B**, 369 (1986).
- [14] I. Barbour, C. Davies, Z. Sabeur, *Phys. Lett. B* **215**, 567 (1988); I. Barbour and Z. Sabeur, *Nucl. Phys.* **B342**, 269 (1990); I. M. Barbour and A.J. Bell, *Nucl. Phys.* **B372**, 385 (1992).
- [15] J. Kogut and L. Susskind, *Phys. Rev. D* **16**, 395 (1975); T. Banks, J. Kogut, and L. Susskind, *Phys. Rev. D* **13**, 1043 (1976); L. Susskind, *Phys. Rev. D* **16**, 3031 (1977); See I. Montvay and G. Münster, *Quantum Fields on a Lattice* (Cambridge University Press, 1994), chapter 4, for an introduction.
- [16] P. Hasenfratz and F. Karsch, *Phys. Lett.* **125B**, 308 (1983).
- [17] N. Kawamoto and J. Smit, *Nucl. Phys.* **B192**, 100 (1981).
- [18] T. Jolicœur, A. Morel and B. Petersson, *Nucl. Phys.* **B274**, 225 (1986).
- [19] S. Hands, A. Kocić and J.B. Kogut, *Ann. Phys.* **224**, 29 (1993)
- [20] See S.P. Klevansky, *Rev. Mod. Phys.* **64**, 649 (1992) for a review.
- [21] S. Hands, S. Kim and J.B. Kogut, *Nucl. Phys.* **B442**, 364 (1995).
- [22] J. Kogut, M.-P. Lombardo, I. Barbour, and S. Morrison (unpublished data).
- [23] S. Kim, A. Kocić and J. Kogut, *Nucl. Phys.* **B429**, 407 (1994).
- [24] H. Kluberg-Stern, A. Morel and B. Petersson, *Nucl. Phys* **B215**, 527 (1983); **B220**, 447 (1983).

FIGURES

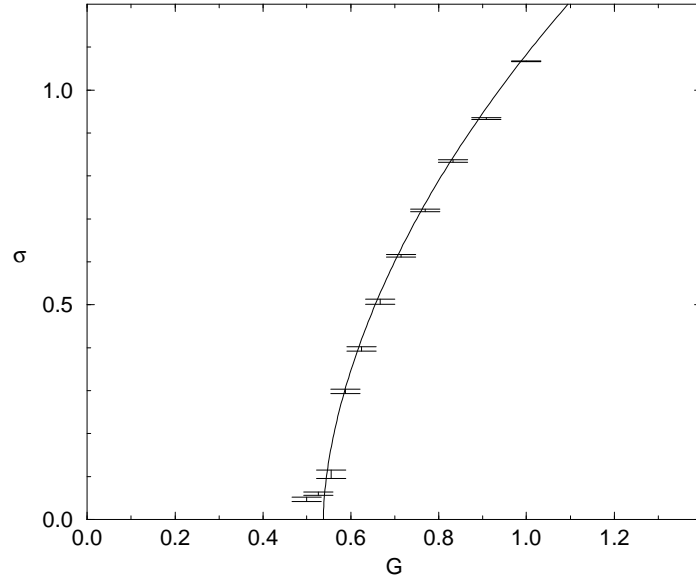


FIG. 1. The solid line shows $\bar{\sigma}$ vs. $G=1/\gamma$ as given by the $\beta \rightarrow \infty$ gap equation at zero chemical potential. The data points are Monte Carlo measurements of $\sqrt{\sigma^2 + \pi^2}$ at zero mass from Ref. [22].

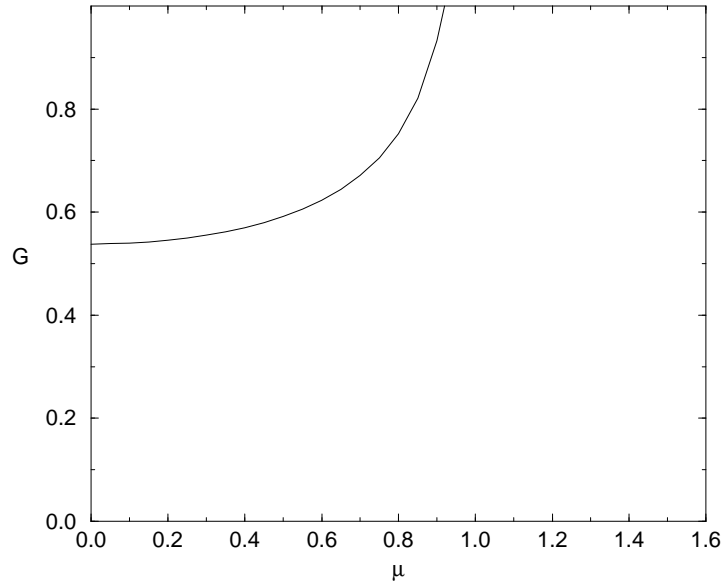


FIG. 2. The mean field phase diagram of χ QCD at $\beta \rightarrow \infty$. Plotted here is the critical line separating the dynamically broken phase, at large G , from the chiral symmetric phase, at small G . $G=1/\gamma$.

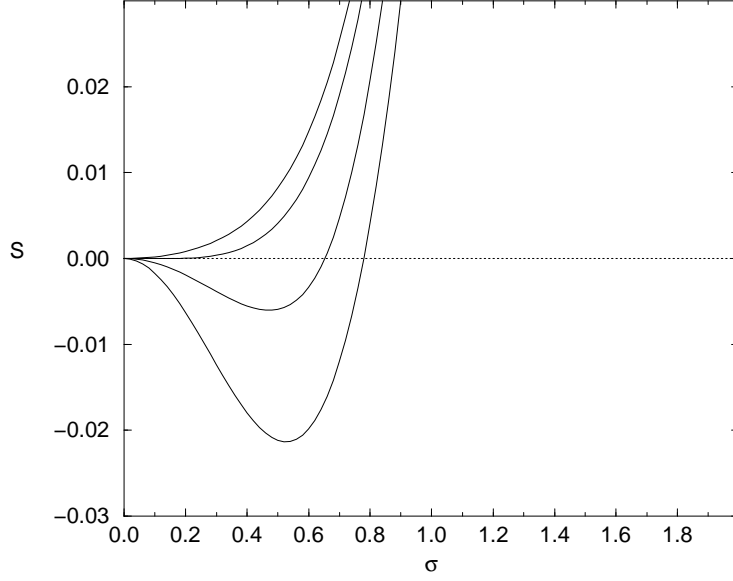


FIG. 3. The $\beta \rightarrow \infty$ effective action of χ QCD plotted as a function of $\bar{\sigma}$, for $\gamma = 1.5$. The different lines are for $\mu=0$, $\mu=.60$, $\mu=.69$, and $\mu=.72$, from bottom to top.

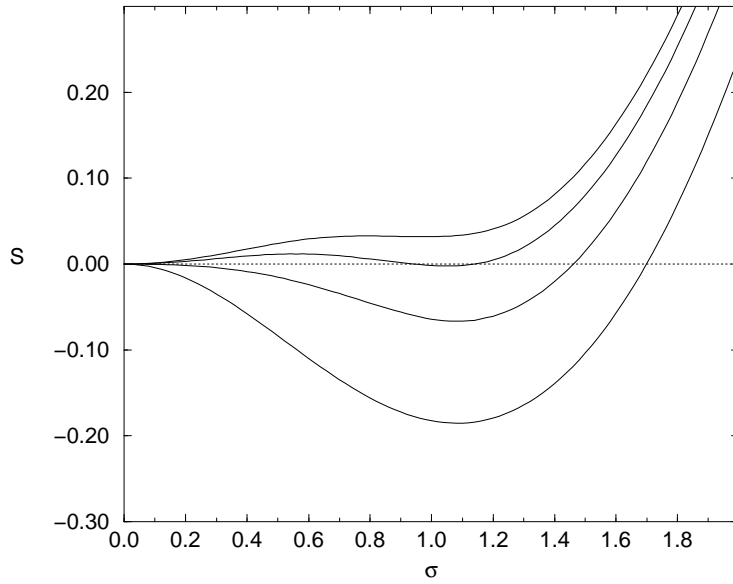


FIG. 4. The $\beta \rightarrow \infty$ effective action of χ QCD plotted as a function of $\bar{\sigma}$, for $\gamma = 1$. The three different lines are for $\mu=0$, $\mu=.90$, $\mu=.97$, and $\mu=1.0$ from bottom to top.

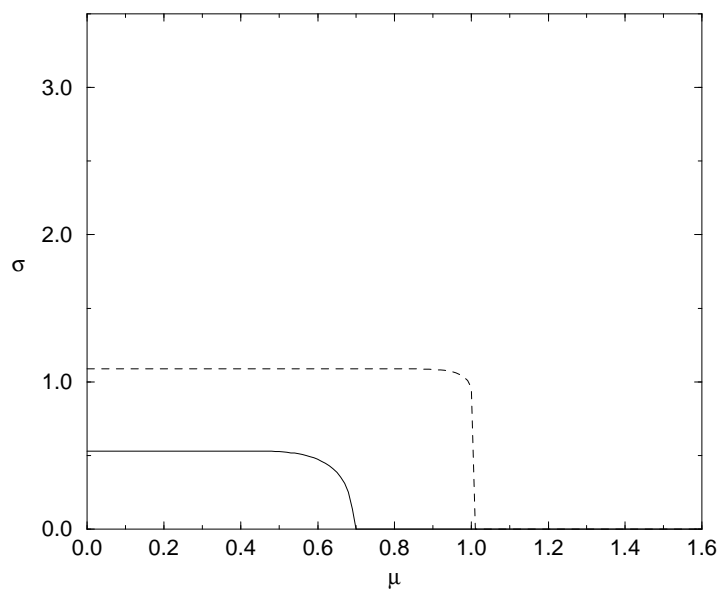


FIG. 5. $\bar{\sigma}$ as a function of the chemical potential at $\beta \rightarrow \infty$ for $\gamma = 1.5$ (solid line) and $\gamma = 1$ (dashed line).

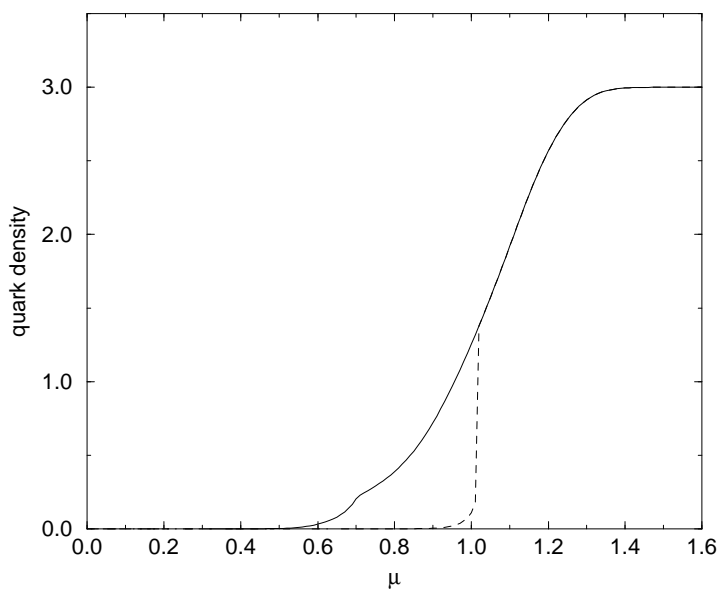


FIG. 6. Plots of the quark density at $\beta \rightarrow \infty$ for $\gamma = 1.5$ (solid line) and $\gamma = 1$ (dashed line), as a function of the chemical potential.

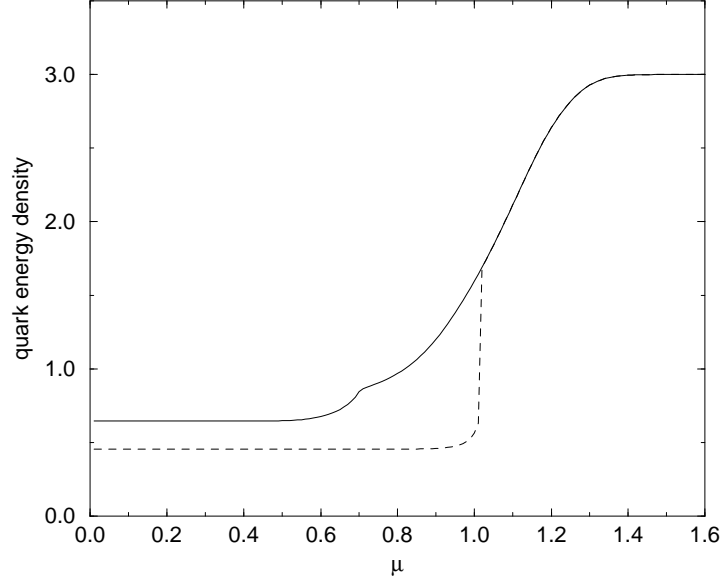


FIG. 7. Plots of the quark energy density at $\beta \rightarrow \infty$ for $\gamma = 1.5$ (solid line) and $\gamma = 1$ (dashed line), as a function of the chemical potential.

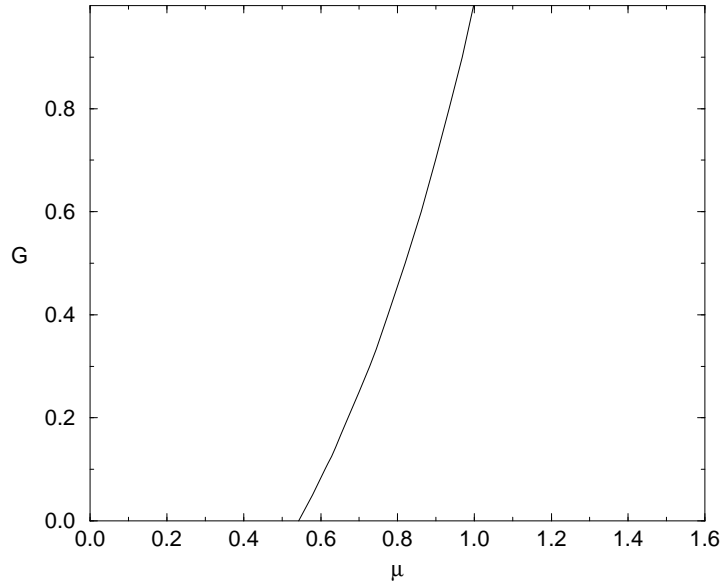


FIG. 8. The mean field phase diagram of χ QCD at $\beta = 0$. The solid line is the critical line separating the dynamically broken phase at small μ , from the chiral symmetric phase at large μ . $G = 1/\gamma$.

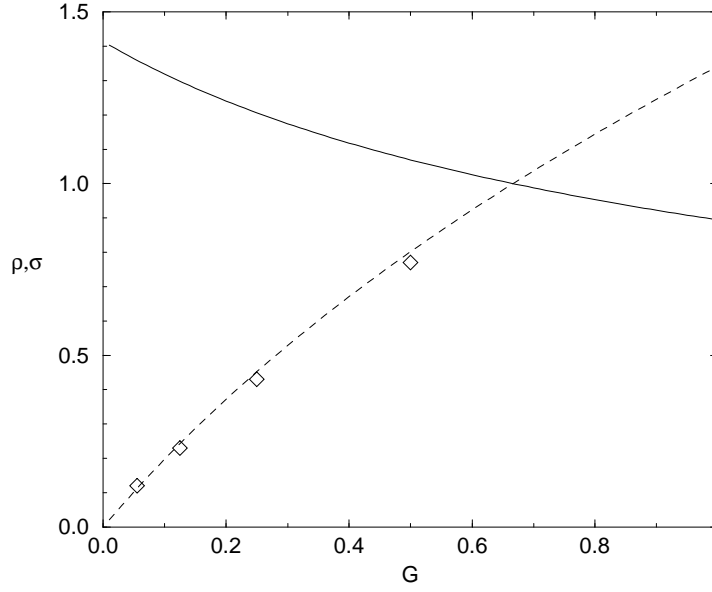


FIG. 9. Mean field values of $\bar{\rho}$ (solid line) and $\bar{\sigma}$ (dashed line) as a function of $G = 1/\gamma$ in the broken phase, at $\beta=0$. The diamonds are Monte Carlo values of σ at $\beta=0.5$ from Ref. [22].

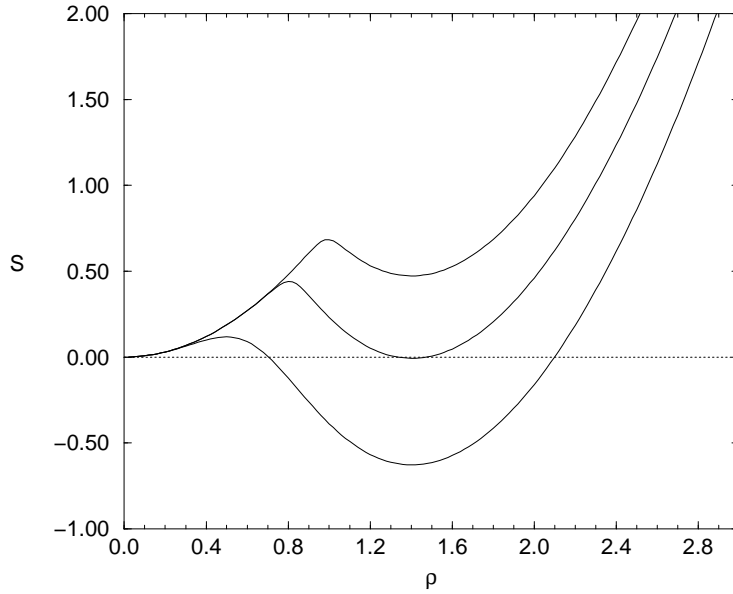


FIG. 10. The $\beta=0$ effective action of χ QCD plotted as a function of $\bar{\rho}$, for $\gamma \rightarrow \infty$. The three different lines are for $\mu=0$, $\mu=.54$ and $\mu=.7$, from bottom to top.

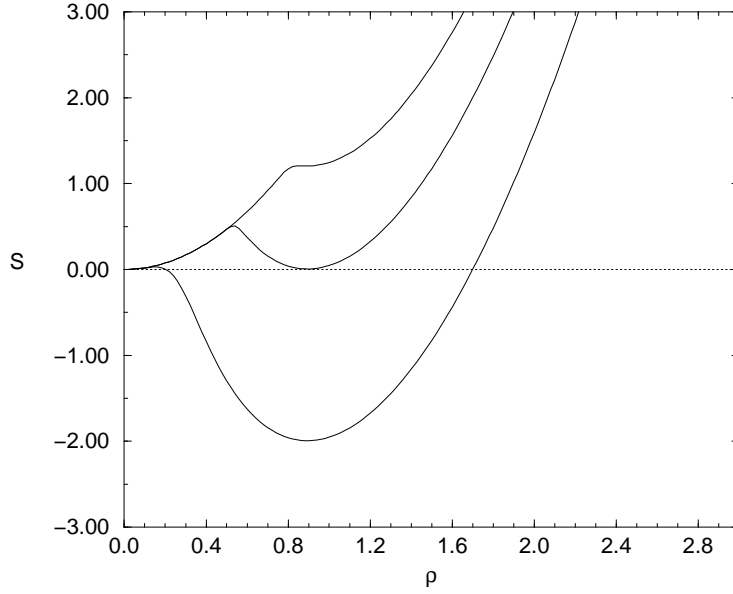


FIG. 11. The $\beta = 0$ effective action of χ QCD plotted as a function of $\bar{\rho}$, at $\gamma = 1$. The three different lines are for $\mu = 0$, $\mu = 1.0$ and $\mu = 1.4$, from bottom to top.

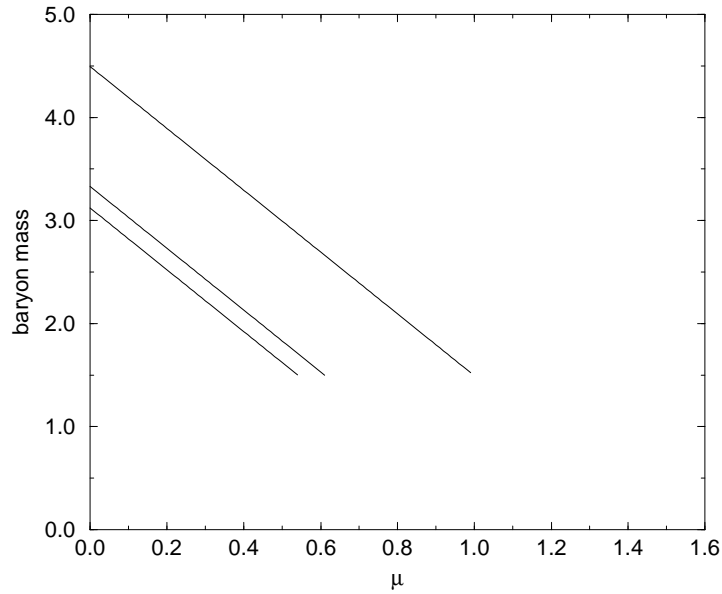


FIG. 12. Plots of the $\beta = 0$ baryon mass as a function of the chemical potential in the broken phase. The three lines are for $\gamma \rightarrow \infty$, $\gamma = 10$, and $\gamma = 1$, from left to right.